identified, particularly in view of the fact that the cytoplasmic tail of CD26 contains only 6 amino acid residues without a common signaling motif structure. Moreover, it has been unclear whether the short cytoplasmic tail is responsible for signal transduction associated with CD26-mediated costimulation. In the present study, using recombinant CD26-CD10 chimeric receptor, we showed that the cytoplasmic tail of CD26 is indeed responsible for T-cell costimulation induced by anti-CD3 plus caveolin-1 (Figure 4D). Furthermore, to explore the proximal signaling molecules interacting with the cytoplasmic tail of dimeric CD26, we used proteomic analyses with Fc fusion proteins containing the cytoplasmic amino acid residues of CD26 (Figures 5A and 5B) to identify that CARMA1 binds to the cytoplasmic tail of dimeric CD26 (Figures 5C). Moreover, we demonstrated here that a PDZ domain in CARMA1 is necessary for binding to CD26 (Figure 5G). The importance of CARMA1 in CD26-mediated costimulation is also shown by rescue experiments using the CARMA1-deficient Jurkat T-cell line JPM50.6 (Figure 6D), and using siRNA against CARMA1 in APB-T-cells (Figure 7E). CARMA1, containing CARD and MAGUK domains, plays an essential role in the NF-κB activation and IL-2 expression induced by CD3-CD28 or CD28-PMA stimulation (18,22). After being phosphorylated, CARMA1 functions as a signaling intermediate downstream of PKCθ and upstream of IKK in the TCR signaling transduction pathway leading to NF-κB activation (39,51). Since MAGUK domain-containing proteins are generally involved in the organization of multiprotein complexes at the interface of the cytoplasmic membrane (52), it is possible that CARMA1 associates with as yet undefined membrane proteins in the immunological synapse of T-cells. In this regard, our present data suggest a novel mechanism for CAMRA1 function as it complexes with Bcl10, and IKK to transduce CD26-costimulatory signals. Moreover, as shown Figure 5C, cytoskeletal proteins were also observed in the complex in the pulldown assays with CD26 AA1-10-Fc. Since MAGUK domain-containing proteins are generally involved in the organization of multiprotein complexes in the cytoskeleton (52), the downstream signaling of CD26 may also be associated with cytoskeletal assembly via CARMA1. The association of CD26, CARMA1 and the cytoskeleton will be elucidated in future studies.

CD26/DDPIV is reported to exist as homodimers, a structural organization which allows access of substrates to DPPIV catalytic activity (36,37). Although DPPIV activity is crucial for CD26-mediated T-cell costimulation (13,30), the exact role played by DPPIV in this process is unclear. Our previous study showed that the enzymatic pocket structure of the DPPIV catalytic site is necessary for binding of CD26 to caveolin-1, leading to the upregulation of CD86 expression on APC (14,15). In the present study, we found that monomeric CD26 H750E, which has a 300-fold decrease in catalytic activity (36), does not bind to CARMA1 (Figure 5E), resulting in loss of CD26-mediated T-cell costimulation by anti-CD3 plus caveolin-1 (Figure 4D). Therefore, dimerization of CD26 is not only necessary for binding to caveolin-1, but also serves as a scaffolding structure for the cytoplasmic signaling molecule CARMA1. The precise binding position of CARMA1 in the cytoplasmic domain of CD26 remains to be elucidated in future work, since PDZ

domains bind primarily to specific C-terminal motifs (X-S/T-X-V/L; X depicts any amino acid) or internal target motifs as well as other PDZ domains (52).

Based upon the present study, we propose the following model to explain the sequence of events leading from CD26-CD3 costimulation to NF-κB activation (Figure 8). In CD3-CD26 costimulation, TCR engagement by peptide-loaded MHC class II presented on APC activates PI3K via phosphorylation of ITAMs (immunoreceptor tyrosine-based activation motifs) in TCR, leading the recruitment of PKCθ and IKK complex in lipid rafts (16,18,25,38). Concomitantly, CD26 ligation by caveolin-1 on APC recruits CD26-interacting CARMA1 to lipid rafts, resulting in the formation of a CARMA1-Bcl10-MALT1-IKK complex, and this membrane-associated Bcl10 complex then activates IKK through ubiquitination of NEMO. Our present study involving Jurkat T-cell lines and human peripheral T-cells represents a different cellular system than those with murine T-cells, where other investigators previously described a role for CD26 in thymic development of murine T-cells (53,54). Our objective with the present study was to define a costimulatory ligand for CD26 and proximal signaling molecule of CD26 in human T-cells, with a future aim of analyzing the *in vivo* role of CD26-mediated T-cell immunity.

In conclusion, we have now demonstrated that CD26 on T-cell surface binds to caveolin-1, hence identifying the first endogenously expressed CD26 costimulatory ligand in the immune system. Moreover, the caveolin-1-CD26 interaction results in strong T-cell costimulation as a result of the recruitment of a molecular complex consisting of CARMA1-Bcl10-MALT1-IKK in lipid rafts. Our findings will therefore serve as a foundation for future insights into the regulation of T-cell costimulation via the CD26 molecule.

ACKNOWLEDGEMENTS

This work was supported by Grant-in-Aid of Ministry of Education, Science, Sports (K.O. and C.M.) and Culture, and Ministry of Health, Labor, and Welfare, Japan (C.M.). K.O. is a recipient of a research grant of Japan Rheumatism Foundation.

REFERENCES

1. Nanus, D. M., Engelstein, D., Gastl, G. A., Gluck, L., Vidal, M. J., Morrison, M., Finstad, C. L., Bander, N. H., and Albino, A. P. (1993) *Proc Natl Acad Sci U S A* **90**(15), 7069-7073
2. Tanaka, T., Camerini, D., Seed, B., Torimoto, Y., Dang, N. H., Kameoka, J., Dahlberg, H. N., Schlossman, S. F., and Morimoto, C. (1992) *J Immunol* **149**(2), 481-486
3. Fox, D. A., Hussey, R. E., Fitzgerald, K. A., Acuto, O., Poole, C., Palley, L., Daley, J. F., Schlossman, S. F., and Reinherz, E. L. (1984) *J Immunol* **133**(3), 1250-1256
4. De Meester, I., Korom, S., Van Damme, J., and Scharpe, S. (1999) *Immunol Today* **20**(8), 367-375
5. Fleischer, B. (1994) *Immunol Today* **15**(4), 180-184

6. Kahne, T., Lendeckel, U., Wrenger, S., Neubert, K., Ansorge, S., and Reinhold, D. (1999) *Int J Mol Med* **4**(1), 3-15

7. Morimoto, C., and Schlossman, S. F. (1998) *Immunol Rev* **161**, 55-70

8. von Bonin, A., Steeg, C., Mittrucker, H. W., and Fleischer, B. (1997) *Immunol Lett* **55**(3), 179-182

9. Eguchi, K., Ueki, Y., Shimomura, C., Otsubo, T., Nakao, H., Migita, K., Kawakami, A., Matsunaga, M., Tezuka, H., and Ishikawa, N. (1989) *J Immunol* **142**(12), 4233-4240

10. Morimoto, C., Torimoto, Y., Levinson, G., Rudd, C. E., Schrieber, M., Dang, N. H., Letvin, N. L., and Schlossman, S. F. (1989) *J Immunol* **143**(11), 3430-3439

11. Dang, N. H., Torimoto, Y., Deusch, K., Schlossman, S. F., and Morimoto, C. (1990) *J Immunol* **144**(11), 4092-4100

12. Hegen, M., Kameoka, J., Dong, R. P., Schlossman, S. F., and Morimoto, C. (1997) *Immunology* **90**(2), 257-264

13. Tanaka, T., Kameoka, J., Yaron, A., Schlossman, S. F., and Morimoto, C. (1993) *Proc Natl Acad Sci U S A* **90**(10), 4586-4590

14. Ohnuma, K., Yamochi, T., Uchiyama, M., Nishibashi, K., Yoshikawa, N., Shimizu, N., Iwata, S., Tanaka, H., Dang, N. H., and Morimoto, C. (2004) *Proc Natl Acad Sci U S A* **101**(39), 14186-14191

15. Ohnuma, K., Yamochi, T., Uchiyama, M., Nishibashi, K., Iwata, S., Hosono, O., Kawasaki, H., Tanaka, H., Dang, N. H., and Morimoto, C. (2005) *Mol Cell Biol* **25**(17), 7743-7757

16. Egawa, T., Albrecht, B., Favier, B., Sunshine, M. J., Mirchandani, K., O'Brien, W., Thome, M., and Littman, D. R. (2003) *Curr Biol* **13**(14), 1252-1258

17. Hara, H., Wada, T., Bakal, C., Kozieradzki, I., Suzuki, S., Suzuki, N., Nghiem, M., Griffiths, E. K., Krawczyk, C., Bauer, B., D'Acquisto, F., Ghosh, S., Yeh, W. C., Baier, G., Rottapel, R., and Penninger, J. M. (2003) *Immunity* **18**(6), 763-775

18. Wang, D., You, Y., Case, S. M., McAllister-Lucas, L. M., Wang, L., DiStefano, P. S., Nunez, G., Bertin, J., and Lin, X. (2002) *Nat Immunol* **3**(9), 830-835

19. Bertin, J., Wang, L., Guo, Y., Jacobson, M. D., Poyet, J. L., Srinivasula, S. M., Merriam, S., DiStefano, P. S., and Alnemri, E. S. (2001) *J Biol Chem* **276**(15), 11877-11882

20. Gaide, O., Martinon, F., Micheau, O., Bonnet, D., Thome, M., and Tschopp, J. (2001) *FEBS Lett* **496**(2-3), 121-127

21. Che, T., You, Y., Wang, D., Tanner, M. J., Dixit, V. M., and Lin, X. (2004) *J Biol Chem* **279**(16), 15870-15876

22. Gaide, O., Favier, B., Legler, D. F., Bonnet, D., Brissoni, B., Valitutti, S., Bron, C., Tschopp, J., and Thome, M. (2002) *Nat Immunol* **3**(9), 836-843

23. Hara, H., Bakal, C., Wada, T., Bouchard, D., Rottapel, R., Saito, T., and Penninger, J. M. (2004) *J Exp Med* **200**(9), 1167-1177

24. Sun, L., Deng, L., Ea, C. K., Xia, Z. P., and Chen, Z. J. (2004) *Mol Cell* **14**(3), 289-301

25. Wang, D., Matsumoto, R., You, Y., Che, T., Lin, X. Y., Gaffen, S. L., and Lin, X. (2004) *Mol Cell Biol* **24**(1), 164-171

26. Zhou, H., Wertz, I., O'Rourke, K., Ultsch, M., Seshagiri, S., Eby, M., Xiao, W., and Dixit, V. M. (2004) *Nature* **427**(6970), 167-171

27. Wegener, E., Oeckinghaus, A., Papadopoulou, N., Lavitas, L., Schmidt-Supprian, M., Ferch, U., Mak, T. W., Ruland, J., Heissmeyer, V., and Krappmann, D. (2006) *Mol Cell* **23**(1), 13-23

28. Niwa, H., Yamamura, K., and Miyazaki, J. (1991) *Gene* **108**(2), 193-199

29. Tanaka, J., Miwa, Y., Miyoshi, K., Ueno, A., and Inoue, H. (1999) *Biochem Biophys Res Commun* **264**(3), 938-943

30. Ohnuma, K., Munakata, Y., Ishii, T., Iwata, S., Kobayashi, S., Hosono, O., Kawasaki, H., Dang, N. H., and Morimoto, C. (2001) *J Immunol* **167**(12), 6745-6755

31. Tanaka, T., Duke-Cohan, J. S., Kameoka, J., Yaron, A., Lee, I., Schlossman, S. F., and Morimoto, C. (1994) *Proc Natl Acad Sci U S A* **91**(8), 3082-3086

32. Nath, D., van der Merwe, P. A., Kelm, S., Bradfield, P., and Crocker, P. R. (1995) *J Biol Chem* **270**(44), 26184-26191

33. Ishii, T., Ohnuma, K., Murakami, A., Takasawa, N., Kobayashi, S., Dang, N. H., Schlossman, S. F., and Morimoto, C. (2001) *Proc Natl Acad Sci U S A* **98**(21), 12138-12143

34. Ciccimarra, F., Rosen, F. S., Schneeberger, E., and Merler, E. (1976) *J Clin Invest* **57**(5), 1386-1390

35. Dang, N. H., Torimoto, Y., Sugita, K., Daley, J. F., Schow, P., Prado, C., Schlossman, S. F., and Morimoto, C. (1990) *J Immunol* **145**(12), 3963-3971

36. Chien, C. H., Huang, L. H., Chou, C. Y., Chen, Y. S., Han, Y. S., Chang, G. G., Liang, P. H., and Chen, X. (2004) *J Biol Chem* **279**(50), 52338-52345

37. Rasmussen, H. B., Branner, S., Wiberg, F. C., and Wagtmann, N. (2003) *Nat Struct Biol* **10**(1), 19-25

38. Lee, K. Y., D'Acquisto, F., Hayden, M. S., Shim, J. H., and Ghosh, S. (2005) *Science* **308**(5718), 114-118

39. Lin, X., and Wang, D. (2004) *Semin Immunol* **16**(6), 429-435

40. Gerli, R., Muscat, C., Bertotto, A., Bistoni, O., Agea, E., Tognellini, R., Fiorucci, G., Cesarotti, M., and Bombardieri, S. (1996) *Clin Immunol Immunopathol* **80**(1), 31-37

41. Muscat, C., Bertotto, A., Agea, E., Bistoni, O., Ercolani, R., Tognellini, R., Spinozzi, F., Cesarotti, M., and Gerli, R. (1994) *Clin Exp Immunol* **98**(2), 252-256

42. Mizokami, A., Eguchi, K., Kawakami, A., Ida, H., Kawabe, Y., Tsukada, T., Aoyagi, T., Maeda, K., Morimoto, C., and Nagataki, S. (1996) *J Rheumatol* **23**(12), 2022-2026

43. Dong, R. P., Tachibana, K., Hegen, M., Scharpe, S., Cho, D., Schlossman, S. F., and Morimoto, C. (1998) *Mol Immunol* **35**(1), 13-21

44. Smart, E. J., Graf, G. A., McNiven, M. A., Sessa, W. C., Engelman, J. A., Scherer, P. E., Okamoto, T.,

and Lisanti, M. P. (1999) *Mol Cell Biol* **19**(11), 7289-7304

45. van der Merwe, P. A., Barclay, A. N., Mason, D. W., Davies, E. A., Morgan, B. P., Tone, M., Krishnam, A. K., Ianelli, C., and Davis, S. J. (1994) *Biochemistry* **33**(33), 10149-10160

46. van der Merwe, P. A., Bodian, D. L., Daenke, S., Linsley, P., and Davis, S. J. (1997) *J Exp Med* **185**(3), 393-403

47. Collins, A. V., Brodie, D. W., Gilbert, R. J., Iaboni, A., Manso-Sancho, R., Walse, B., Stuart, D. I., van der Merwe, P. A., and Davis, S. J. (2002) *Immunity* **17**(2), 201-210

48. Ohnuma, K., Ishii, T., Iwata, S., Hosono, O., Kawasaki, H., Uchiyama, M., Tanaka, H., Yamochi, T., Dang, N. H., and Morimoto, C. (2002) *Immunology* **107**(3), 325-333

49. von Bonin, A., Huhn, J., and Fleischer, B. (1998) *Immunol Rev* **161**, 43-53

50. Chen, C. Y., Cordeaux, Y., Hill, S. J., and King, J. R. (2003) *Bull Math Biol* **65**(5), 933-958

51. Thome, M. (2004) *Nat Rev Immunol* **4**(5), 348-359

52. Dimitratos, S. D., Woods, D. F., Stathakis, D. G., and Bryant, P. J. (1999) *Bioessays* **21**(11), 912-921

53. Marguet, D., Bernard, A. M., Vivier, I., Darmoul, D., Naquet, P., and Pierres, M. (1992) *J Biol Chem* **267**(4), 2200-2208

54. Yan, S., Marguet, D., Dobers, J., Reutter, W., and Fan, H. (2003) *Eur J Immunol* **33**(6), 1519-1527

LEGENDS TO FIGURES

Figure 1. Expression and purification of caveolin-1 human IgG_1 fusion proteins.

(A) Schematic diagrams of human caveolin-1 and its Fc fusion proteins.

In human caveolin-1, AA1-82 comprises the N-terminal domain (NT); AA82-101, the scaffolding domain (SCD); AA101-134, membrane spanning domain (MS); and AA134-178, the C-terminal domain (CT). SP (huECD) depicts the signal peptide of human E-cadherin. At the 3' portion, the hinge (H), CH2 and CH3 domains of human IgG_1 Fc are also indicated (Fcγ1).

(B) The expressed fusion proteins were purified as described in Experimental Procedures. Aliquots (5μg) of control human IgG (lanes 1 and 5), Fcγ1 (lanes 2 and 6), Fc fusion proteins of the N-terminal region of human caveolin-1 (NT-Fc) (lanes 3 and 7), and Fc fusion proteins of the N-terminal region with the scaffolding domain of human caveolin-1 being deleted (NTΔSCD-Fc) (lanes 4 and 8) were subjected to SDS-PAGE (5-20% acrylamide gradient gel) under reducing (+2ME, lanes 2-4) or non-reducing (-2ME, lanes 5-8) conditions. Molecular weight markers are depicted in '*Mr*'. Proteins were visualized by staining with Coomasie Brilliant Blue.

(C) Aliquots (50ng) of Fcγ1 (lanes 1 and 4), NT-Fc (lanes 2 and 5), and NTΔSCD-Fc (lanes 3 and 6) were subjected to SDS-PAGE (5-20% acrylamide gradient gel) under reducing (+2ME, lanes 1-3) or non-reducing

(-2ME, lanes 4-6) conditions, followed by Western blot analysis, using HRP conjugated anti-human IgG.

Figure 2. Fc fusion proteins of the N-terminal region of human caveolin-1 (NT-Fc) binds to CD26 and induces IL-2 production.

(A) Lysates of J.CD26wt cells (500μg) were precleared with Fcγ1 and protein A-sepharose beads, and immunoprecipitation (IP) assays were conducted with Fcγ1 (lane 1), NT-Fc (lane 2), or NTΔSCD (lane 3) (each at 2μg). IP complexes were then separated using 5-20% SDS-PAGE, followed by immunoblotted with anti-CD26 mAb (upper panel). An aliquot (50μg) of the input lysate was also analyzed (lane 4). The membrane was stripped and reprobed with HRP conjugated anti-human IgG (lower panel). Similar results were obtained in three independent experiments.

(B) J.CD26wt cells were used for binding activity of Fc fusion proteins. Panel (a): the forward and side scatter grams of the analyzed cells. Solid circle indicates the gated region for analysis. Panel (b): Cells were stained with FITC-conjugated control mouse IgG (1), or FITC-conjugated anti-CD26 mAb (2). For blocking assay, cells were first reacted with unlabeled anti-CD26 mAb (3), or unlabeled control mouse IgG (4), followed by staining as described in (2). Panel (c): Cells were stained with biotinylated Fcγ1 as control (1), or biotinylated NT-Fc (2), followed by reaction with FITC-conjugated streptavidin. For blocking assay, cells were first reacted with unlabeled anti-CD26 mAb (3), or unlabeled control IgG (4), followed by staining as described in (2). Panel (d): Cells were stained with biotinylated Fcγ1 as control (1), or biotinylated NTΔSCD-Fc (2), followed by reaction with FITC-conjugated streptavidin. For blocking assay, cells were first reacted with unlabeled anti-CD26 mAb (3), or unlabeled control IgG (4), followed by staining as described in (2). All four histograms in panel (d) were stacked in the same position.

(C) Measuring the affinity of Fc fusion proteins to recombinant soluble CD26 (rsCD26) by equilibrium binding. Injections of rsCD26 at 25°C started at 50nM and were followed by five two-fold dilutions (50nM, 25nM, 12.5nM, 6.3nM, 3.2nM, and 1.6nM), flowing over Fcγ1 (a), NT-Fc (b), or NTΔSCD-Fc (c) immobilized at a concentration of 6032 response units (RU), 4996 RU, or 4852 RU, respectively. The curves represent total specific binding after subtraction of the background responses observed in a control flow cell.

(D) Native Jurkat (JKTwt) or J.CD26wt were stimulated with immobilized antibodies and/or Fc fusion proteins (anti-CD3, 1.0μg/ml; anti-CD28, anti-CD26, Fcγ1, NT-Fc, NTΔSCD-Fc, each at 10μg/ml). After culturing for 48 hours, culture supernatants were pooled from the triplicate wells and assayed for IL-2 content. Values shown are means ± S.E. of determinations from triplicate cultures of three independent experiments. * and *** show points of significant increase ($p<0.05$), whereas ** and # indicate points of no significant change compared to controls.

(E) Following blocking with soluble anti-CD26, anti-CD28 or control mouse IgG, J.CD26wt cells were stimulated and IL-2 was measured as described in (D). Values shown are means ± S.E. of determinations from triplicate cultures of three independent experiments. * and ** show results of significant inhibition obtained following blocking by anti-CD26 mAb ($p<0.05$), and # and ## show results of no significant inhibition obtained

following blocking by anti-CD28 mAb.

Figure 3. NT-Fc is costimulatory with anti-CD3 for proliferation of peripheral blood T-cells.

(A) Purified T-cells were stimulated with immobilized antibodies and/or Fc fusion proteins (anti-CD3, 0.05μg/ml; anti-CD28, anti-CD26, Fcγ1, NT-Fc, NTΔSCD-Fc, each at 5μg/ml). Proliferation was measured by uptake of [^{3}H]-thymidine (TdR) as described in Experimental Procedures. Values shown are means ± S.E. of determinations from triplicate cultures of five independent donors. * shows points of significant increase ($p<0.05$), whereas ** indicates points of no significant change compared to controls.

(B) Purified T-cells were stimulated with immobilized Fc fusion proteins at indicated concentrations in the presence of immobilized anti-CD3 (0.05μg/ml). Proliferation was measured as described in (A). Values shown are means ± S.E. of determinations from triplicate cultures of five independent donors. * shows points of significant increase ($p<0.05$) compared to control.

(C) Purified T-cells were cultured in the presence of anti-CD3 (0.05μg/ml) in solution, with varying amounts of CHO transfectants which were fixed with 0.05% glutaraldehyde. Cav-wt$^+$ CHO, Cav-ΔSCD$^+$ CHO, or mock$^+$ CHO represent CHO cells stably transfected with GFP-full length caveolin-1, GFP-caveolin-1 with the scaffolding domain deleted, or GFP expressing vector, respectively. Proliferation was measured as described in (A). Values shown are means ± S.E. of determinations from triplicate cultures of five independent donors. * shows points of significant increase ($p<0.05$) compared to control.

(D) Following blocking with soluble anti-CD26, anti-CD28 or control mouse IgG, T-cells were stimulated and proliferation was measured as described in Figure 3A. Values shown are means ± S.E. of determinations from triplicate cultures of five independent donors. * and *** show results of significant inhibition obtained following blocking by anti-CD26 mAb ($p<0.05$), and ** shows results of significant inhibition obtained following blocking by anti-CD28 mAb ($p<0.05$).

(E) Following incubation and blocking with increasing doses (0, 0.5, 5.0, 10.0, 20.0, and 50μg/ml) of soluble anti-CD26 mAbs, anti-CD28 mAbs or control mouse IgG, T-cells were stimulated by plate-bound anti-CD3 (0.05μg/ml) plus NT-Fc (5μg/ml) and proliferation was measured as described in Figure 3A. Values shown are means ± S.E. of determinations from triplicate cultures of five independent donors. * shows points of significant decrease ($p<0.05$) compared to controls.

Figure 4. The cytoplasmic tail of dimeric CD26 is necessary for anti-CD3 plus caveolin-1 costimulation.

(A) Jurkat T-cells stably transfected with V5-tagged full-length CD26 (CD26wt), CD26-CD10 chimeric receptor (CD26+CD10 cyto), or monomeric CD26 (CD26 H750E) were generated as described in Experimental Procedures. Cell lysates were resolved in SDS-PAGE under reducing (+2ME) (lanes 1-4), or non-reducing (-2ME) conditions (lanes 5-8), and immunoblotted with anti-CD26 mAb. In non-reducing conditions, arrow head shows bands of dimeric CD26 (lanes 6 and 7), and arrow indicates bands of monomeric CD26 (lane 8).

(B) Cells were lysed and immunoprecipitated with anti-V5 mAb. IPs were resolved in 5-20% gradient SDS-PAGE under reducing conditions, immunoblotted with anti-CD26 mAb. IgH indicates immunoglobulin heavy chain.

(C) Dot plots for expression of cell surface CD3 and CD26. % positive of CD3 is shown in mock-vector transfected Jurkat (panel (a)), and % positive of CD3 and CD26 is shown in other transfectants (panels (b)-(d)).

(D) Jurkat transfectans, which were stably transfected with full-length CD26 (CD26wt), CD26-CD10 chimeric receptor (CD26+CD10 cyto), or CD26 containing mutation of histidine residue at amino acid 750 for glutamic acid (CD26 H750E), were stimulated with plate-bound anti-CD3 (1.0μg/ml) in the presence or absence of plate-bound NT-Fc (10μg/ml), or PMA (10ng/ml). Panel (a): Following 48 hours of culture, IL-2 concentration of the culture supernatant was measured by ELISA. Values shown are means ± S.E. of determinations from triplicate cultures. * shows points of significant increase ($p<0.05$) compared to control. Panel (b): Jurkat transfectants were stimulated as described in panel (a), and harvested for extraction of nuclear proteins, subjected to ELISA-based DNA-binding protein assay. Binding activity to p65 NF-κB component was revealed by OD value at 450 nm. Data represent mean ± S.E. from triplicate experiments. * shows a point of significant increase ($p<0.05$).

Figure 5. The cytoplasmic tail of dimeric CD26 is associated with CARMA1.

(A) Schematic diagram of Fc fusion proteins of the cytoplasmic tail of CD26 (CD26 AA1-10). 'MKTPWKVLLG' depicts amino acid residues of human CD26 at 1-10 positions. At the 3' portion, the hinge (H), CH2 and CH3 domains of human IgG_1 Fc are also indicated (Fcγ1).

(B) The expressed fusion proteins were purified as described in Experimental Procedures. Aliquots (5μg) of control human IgG (lanes 1 and 4), Fcγ1 (lanes 2 and 5), and CD26 AA1-10-Fc (lanes 3 and 6) were subjected to SDS-PAGE under reducing (+2ME, lanes 1-3) or non-reducing (-2ME, lanes 4-6) conditions. Molecular weight markers are depicted in '*Mr*'. Proteins were visualized by staining with Coomasie Brilliant Blue.

(C) An aliquot (50μg) of Jurkat lysates was separated by 2D-PAGE using pH3.0-10NL (non-linear) IPG (isoelectric focusing of proteins using immobilized pH gradient) stripped in the first dimension and 4-12% SDS-PAGE, and the gels were stained with Coomasie Brilliant Blue (panel (a)). Aliquots (1mg) of lysates were precleared by human IgG (2μg) and proteins A-sepharose, followed by immunoprecipitation with Fcγ1 (1μg) (panel (b)), or CD26 AA1-10-Fc (1μg) (panel (c)). IPs were analyzed by 2-D PAGE, and six spots were clearly detected in IP complex of CD26 AA1-10-Fc (1-6 in panel (c)). * and ** were spots of Fcγ1 and CD26-Fc (AA1-10), respectively. Similar results were obtained in five independent experiments, and the panels shown are the representative results.

(D) J.CD26wt were lysed, and immunoprecipitation (IP) assays were conducted with anti-CARMA1 pAb (goat), anti-CD26 mAb (mouse (ms)) or control Ig (cIgG). IP complexes as well as 10% of input lysates were then separated using SDS-PAGE, immunoblotted with indicated antibodies. Similar results were obtained in three

independent experiments.

(E) 293FT cells were transiently transfected with V5-tagged full-length CD26 (CD26wt), CD26-CD10 chimeric receptor (CD26+CD10 cyto), or CD26 containing mutation of histidine residue at amino acid 750 for glutamic acid (CD26 H750E), together with Xpress-tagged full-length CARMA1 (CARMA1wt). Cells were lysed with TBSD buffer and immunoprecipitated with anti-V5 mAb. IPs were separated using 5-20% SDS-PAGE, and immunoblotted with anti-Xpress mAb (upper panel), followed by stripping and reprobing with anti-V5 mAb (lower panel). Similar results were obtained in three independent experiments.

(F) Schematic diagrams of Xpress-tagged CARMA1 and its deletion mutants; CARAM1 wt, Xpress-tagged full length-CARMA1; CARMA1 1-742, Xpress-tagged CARMA1 minus the SH3+GUK domains; CARMA1 1-660, Xpress-tagged CARMA1 minus the PDZ+SH3+GUK domains.

(G) 293FT cells were transiently transfected with Xpress-tagged CARMA1wt, CARMA1 with the SH3+GUK domains deleted (1-742), or CARMA1 with the PDZ+SH3+GUK domains deleted (1-660), together with V5-tagged CD26wt. Cells were lysed with TBSD buffer and immunoprecipitated with anti-Xpress mAb. IPs were separated using SDS-PAGE, and immunoblotted with anti-V5 mAb (upper panel), followed by stripping and reprobing with anti-Xpress mAb (lower panel). Similar results were obtained in three independent experiments.

Figure 6. CARMA1 is necessary for CD26-mediated costimulation by caveolin-1

(A) Cell lysates of native Jurkat, J.CD26wt or JPM50.6 were resolved in SDS-PAGE under reducing conditions, followed by immunoblotting with anti-CD26 mAb (upper panel) or anti-CARMA1 pAb (lower panel).

(B) JPM50.6 cells stably transfected with V5-tagged full-length CD26 (CD26wt) and /or Xpress-tagged full-length CARMA1 (CARMA1wt) or CARMA1 with the PDZ+SH3+GUK domains deleted (CARMA1 (1-660)) were generated as described in Experimental Procedures. Lysates were resolved in SDS-PAGE, immunoblotted with anti-Xpress mAb (CARMA1) (upper panel) or anti-V5 mAb (CD26) (lower panel).

(C) Dot plots for cell surface expression of CD3 and CD26. % positive of CD3 is shown in mock-vector transfected JPM (panel (a)) and CARMA1-transfected JPM 50.6 (panel (c)), and % positive of CD3 and CD26 is shown in other transfectants (panels (b), (d) and (e)).

(D) JPM50.6 transfectants, which were described in (B), were stimulated with plate-bound anti-CD3 in the presence or absence of plate-bound NT-Fc as described in Figure 4D. Panel (a): Following 48 hours of culture, IL-2 concentration of the culture supernatant was measured by ELISA. Values shown are means ± S.E. of determinations from triplicate cultures. * shows points of significant increase ($p<0.05$) compared to control. Panel (b): JPM50.6 transfectants were stimulated as described in panel (a), and harvested for NE. Each 5μg of NE was subjected to ELISA-based DNA-binding protein assay. Binding activity to p65 NF-κB component was revealed by OD value at 450 nm. Data represent mean ± S.E. from triplicate experiments. * shows a point of significant increase ($p<0.05$). Xpress vec. or V5 vec. depicts pcDNA4/HisMax or pEF6/V5 empty vector as a mock, respectively.

Figure 7. CARMA1 plays an important role in CD26-mediated costimulation by caveolin-1 in human peripheral blood T-cells.

(A) Purified T-cells were lysed, and immunoprecipitation (IP) assays were conducted with anti-CARMA1 pAb (goat), anti-CD26 mAb (mouse (ms)) or control Ig (cIgG). IP complexes as well as 10% of input lysates were then separated using SDS-PAGE, immunoblotted with indicated antibodies. Similar results were obtained in three independent experiments.

(B) Purified T-cells were stimulated for 10 minutes with anti-CD3 alone (0.05μg/ml), or with anti-CD3 plus NT-Fc (5.0μg/ml), and lysates were prepared by sucrose gradient centrifugation as described in Experimental Procedures. The distribution of CD26, CARMA1, Bcl10, and IKKβ was determined by immunoblotting with specific antibodies. Similar results were obtained in three independent experiments.

(C) Purified T-cells were stimulated for 0, 10, and 30 minutes with anti-CD3 plus NT-Fc, and lysates were prepared by sucrose gradient centrifugation as described in Experimental Procedures. The distribution of CD26, CARMA1, Bcl10, and IKKβ was determined by immunoblotting with specific antibodies. Similar results were obtained in three independent experiments.

(D) Purified T-cells were stimulated with anti-CD3 alone (lanes 1 and 2), or with anti-CD3 plus NT-Fc (lanes 3 and 4), and lipid raft fractions were prepared as described in (A) and immunoprecipitation of lipid rafts with control IgG (cIgG) (lanes 1 and 3) or anti-CD26 mAb (lanes 2 and 4) was performed as described in Experimental Procedures. IPs were resolved in SDS-PAGE, and immunoblotted with indicated antibodies. Similar results were obtained in three independent experiments.

(E) Purified T-cells were transfected with sense-siRNA (ss1 and ss2) of CARMA1 gene or mismatched siRNA (control), using HVJ-E vector. Cell lysates were resolved by SDS-PAGE, and immunoblotted with indicated antibodies, followed by stripping and reprobing with anti-ß-actin antibody (insisde box). Purified T-cells treated with siRNA were stimulated, and subjected to T-cell proliferation assay as described in Figure 3A. Values shown are means ± S.E. of determinations from triplicate cultures of five independent donors. * shows points of significant decrease ($p<0.05$), whereas ** indicates points of no significant change compared to controls.

Figure 8. A model for signaling by TCR and CD26 costimulation.

Stimulation of cells through TCR complexes leads to phosphorylation of cytoplasmic ITAMs by ligation of peptide-loaded MHC class II (bold arrows) and recruitment and activation of PI3K and PKCθ (gray arrow head). Meanwhile, caveolin-1, of which the N-terminal extracellular regions are presented on antigen-loaded APC, ligates CD26 which exists as dimers on the cell surface, and recruits lipid rafts (gray arrows) while interacting with CARMA1 (gray double-headed arrow). The recruitment of CARMA1 along with CD26 to lipid rafts also recruits the CARMA1-Bcl10-IKKs complex (black double-headed arrows), leading to activation of the IKK complex (black double-headed arrows), and finally, activation of NF-κB.

Figure 1

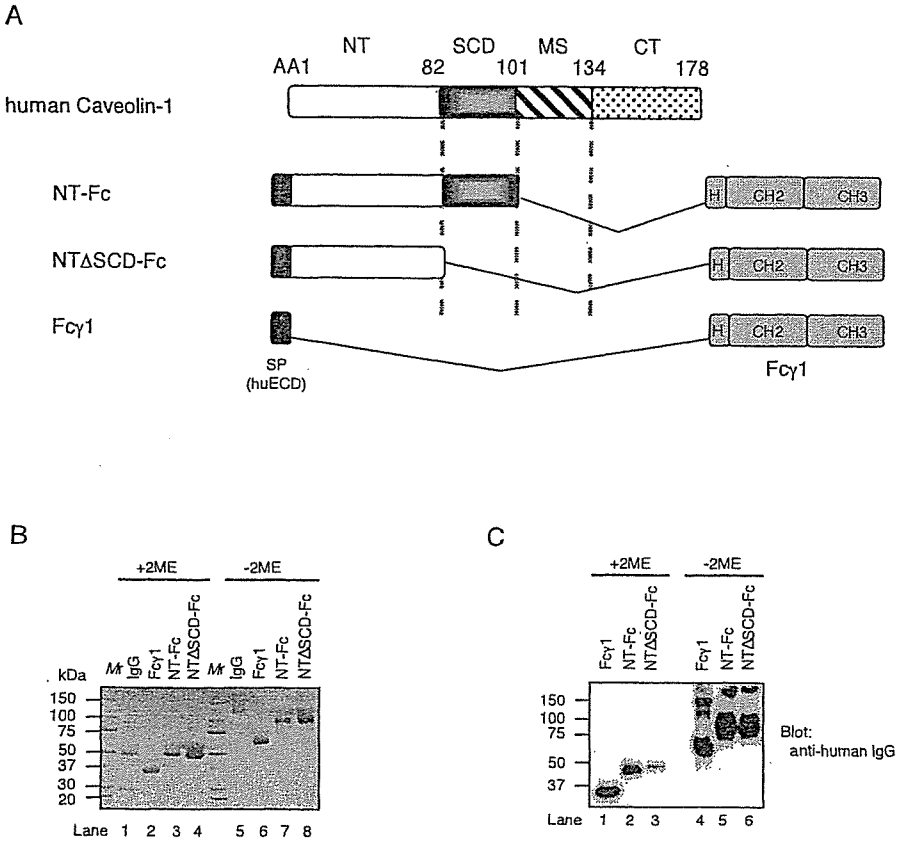
A
NT
SCD
MS
CT
AA1
82
101
134
178
human Caveolin-1
NT-Fc
NTΔSCD-Fc
Fcγ1
H
CH2
CH3
SP
(huECD)
Fcγ1
B
+2ME
-2ME
kDa
Mr
IgG
Fcγ1
NT-Fc
NTΔSCD-Fc
150
100
75
50
37
30
20
Lane 1 2 3 4 5 6 7 8
C
+2ME
-2ME
Fcγ1
NT-Fc
NTΔSCD-Fc
150
100
75
50
37
Blot:
anti-human IgG
Lane 1 2 3 4 5 6

Figure 2

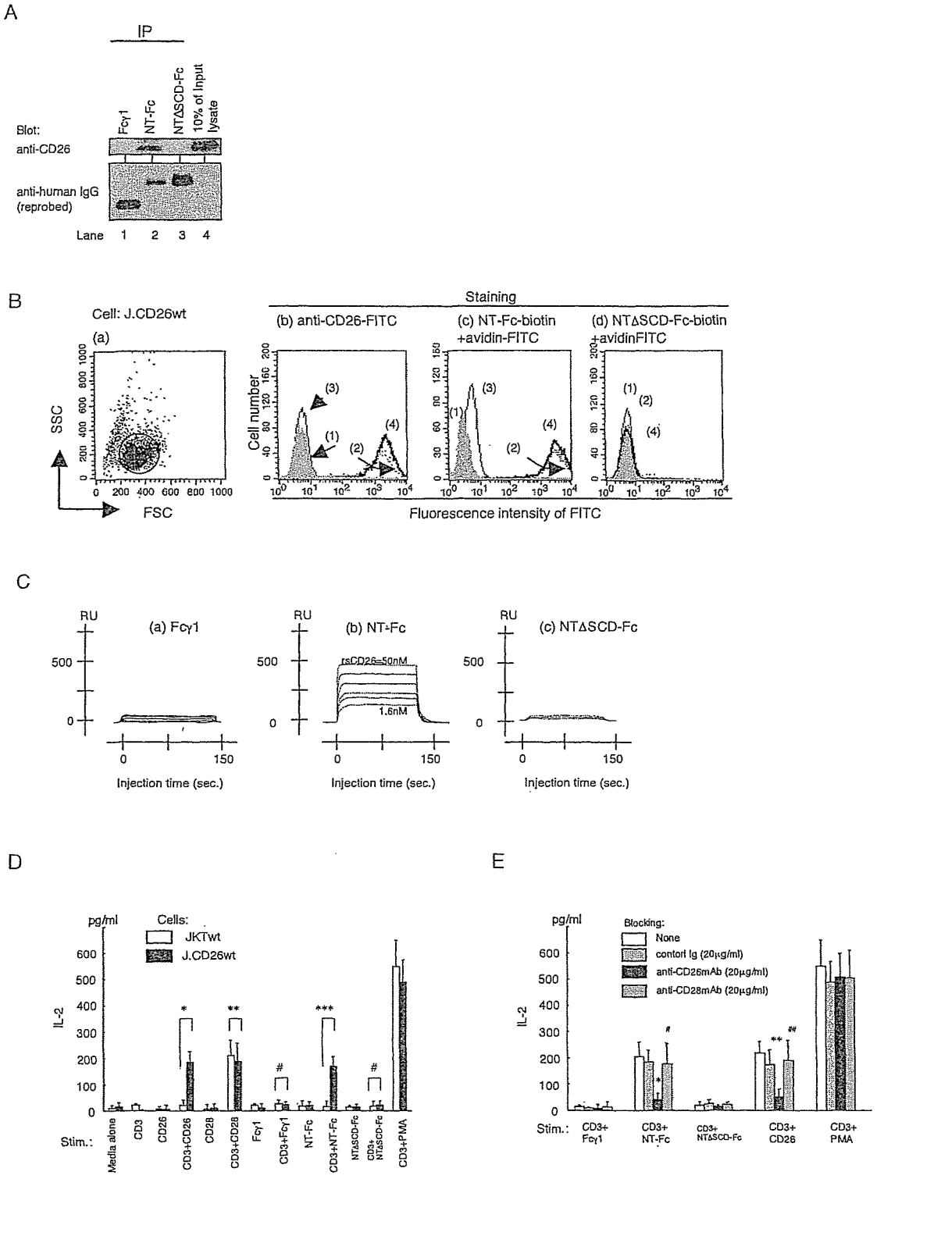
A
IP
Fcγ1
NT-Fc
NTΔSCD-Fc
10% of Input lysate
Blot:
anti-CD26
anti-human IgG (reprobed)
Lane 1 2 3 4
B
Cell: J.CD26wt
(a)
SSC
FSC
Staining
(b) anti-CD26-FITC
(c) NT-Fc-biotin +avidin-FITC
(d) NTΔSCD-Fc-biotin +avidinFITC
Cell number
Fluorescence intensity of FITC
C
RU
(a) Fcγ1
(b) NT-Fc
(c) NTΔSCD-Fc
rsCD26=50nM
1.6nM
Injection time (sec.)
D
pg/ml
Cells:
JKTwt
J.CD26wt
IL-2
Stim.:
Media alone
CD3
CD26
CD3+CD26
CD28
CD3+CD28
Fcγ1
CD3+Fcγ1
NT-Fc
CD3+NT-Fc
NTΔSCD-Fc
CD3+ NTΔSCD-Fc
CD3+PMA
E
pg/ml
Blocking:
None
control Ig (20μg/ml)
anti-CD26mAb (20μg/ml)
anti-CD28mAb (20μg/ml)
IL-2
Stim.:
CD3+ Fcγ1
CD3+ NT-Fc
CD3+ NTΔSCD-Fc
CD3+ CD26
CD3+ PMA

Figure 3

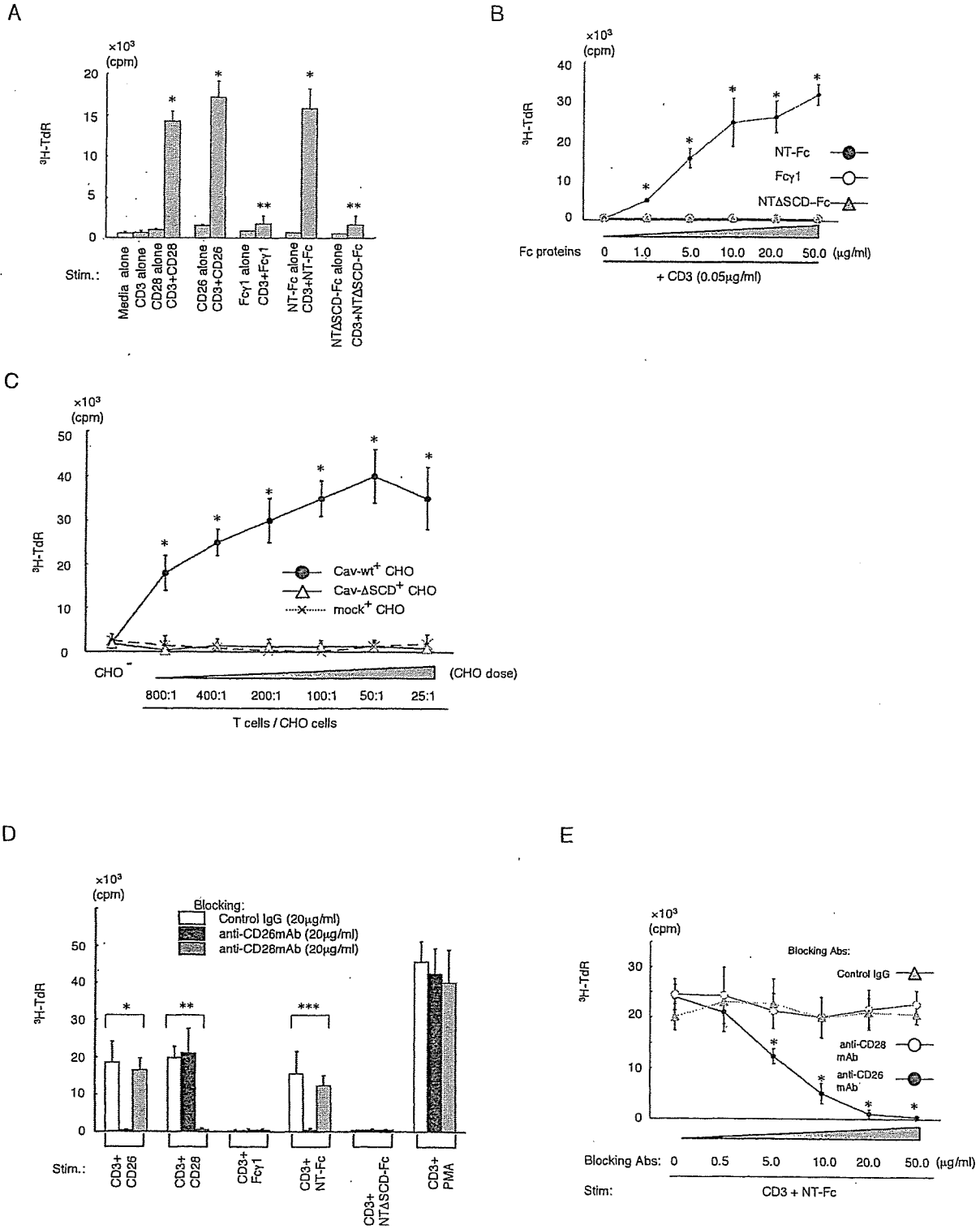
A
×10³ (cpm)
³H-TdR
Stim.:
Media alone
CD3 alone
CD28 alone
CD3+CD28
CD26 alone
CD3+CD26
Fcγ1 alone
CD3+Fcγ1
NT-Fc alone
CD3+NT-Fc
NTΔSCD-Fc alone
CD3+NTΔSCD-Fc
B
NT-Fc
Fcγ1
NTΔSCD-Fc
Fc proteins
+ CD3 (0.05μg/ml)
(μg/ml)
C
Cav-wt+ CHO
Cav-ΔSCD+ CHO
mock+ CHO
CHO⁻
(CHO dose)
T cells / CHO cells
D
Blocking:
Control IgG (20μg/ml)
anti-CD26mAb (20μg/ml)
anti-CD28mAb (20μg/ml)
CD3+ CD26
CD3+ CD28
CD3+ Fcγ1
CD3+ NT-Fc
CD3+ NTΔSCD-Fc
CD3+ PMA
E
Blocking Abs:
Control IgG
anti-CD28 mAb
anti-CD26 mAb
Blocking Abs:
Stim:
CD3 + NT-Fc

Figure 4

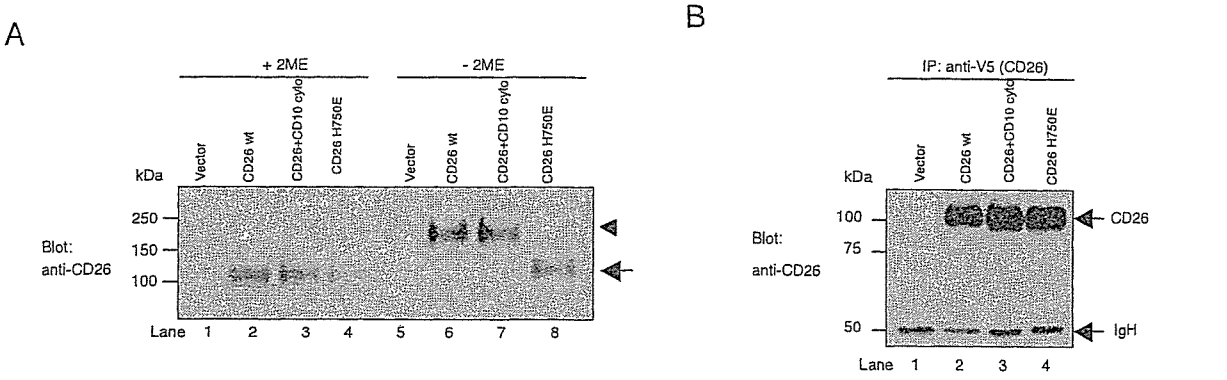
A
+ 2ME
- 2ME
Vector
CD26 wt
CD26+CD10 cyto
CD26 H750E
kDa
250
150
100
Blot:
anti-CD26
Lane 1 2 3 4 5 6 7 8
B
IP: anti-V5 (CD26)
100
75
50
CD26
IgH
Lane 1 2 3 4

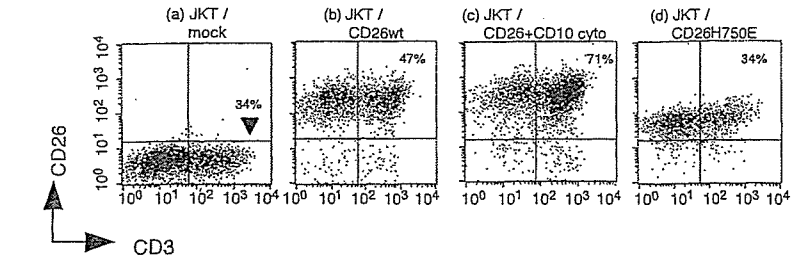
C
(a) JKT / mock
(b) JKT / CD26wt
(c) JKT / CD26+CD10 cyto
(d) JKT / CD26H750E
34%
47%
71%
34%
CD26
CD3

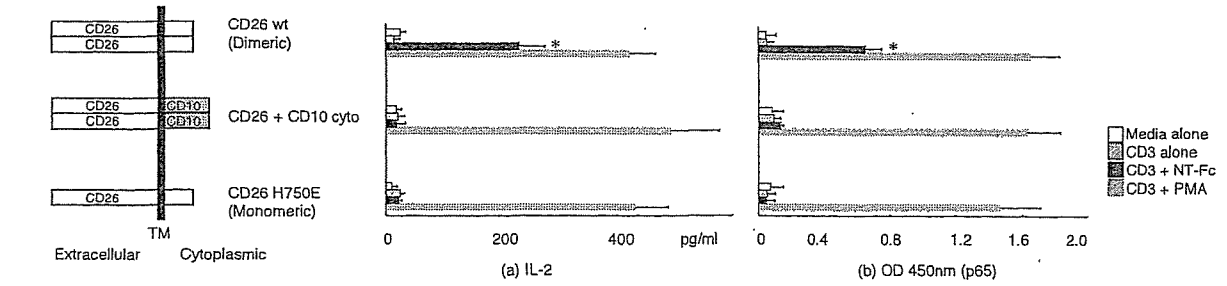
D
CD26 wt (Dimeric)
CD26 + CD10 cyto
CD26 H750E (Monomeric)
TM
Extracellular
Cytoplasmic
0
200
400
pg/ml
(a) IL-2
0
0.4
0.8
1.2
1.6
2.0
(b) OD 450nm (p65)
Media alone
CD3 alone
CD3 + NT-Fc
CD3 + PMA

Figure 5

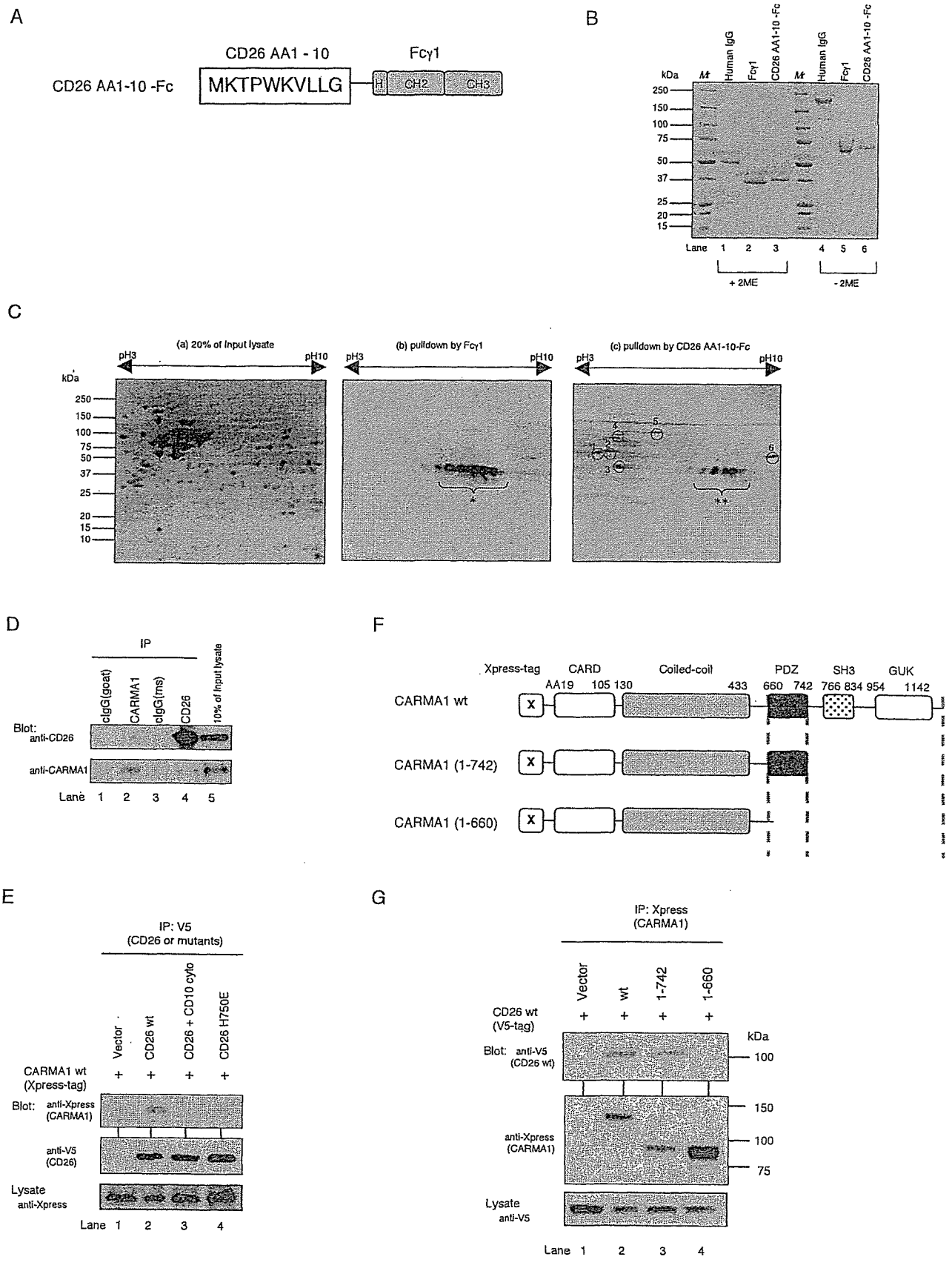
A
CD26 AA1 - 10
Fcγ1
CD26 AA1-10 -Fc
MKTPWKVLLG
H
CH2
CH3
B
kDa
M
Human IgG
Fcγ1
CD26 AA1-10 -Fc
250
150
100
75
50
37
25
20
15
Lane 1 2 3 4 5 6
+ 2ME
- 2ME
C
(a) 20% of Input lysate
(b) pulldown by Fcγ1
(c) pulldown by CD26 AA1-10-Fc
pH3
pH10
kDa
250
150
100
75
50
37
25
20
15
10
D
IP
cIgG(goat)
CARMA1
cIgG(ms)
CD26
10% of Input lysate
Blot:
anti-CD26
anti-CARMA1
Lane 1 2 3 4 5
F
Xpress-tag
CARD
Coiled-coil
PDZ
SH3
GUK
AA19 105 130 433 660 742 766 834 954 1142
CARMA1 wt
CARMA1 (1-742)
CARMA1 (1-660)
X
E
IP: V5
(CD26 or mutants)
Vector
CD26 wt
CD26 + CD10 cyto
CD26 H750E
CARMA1 wt
(Xpress-tag)
+
Blot:
anti-Xpress
(CARMA1)
anti-V5
(CD26)
Lysate
anti-Xpress
Lane 1 2 3 4
G
IP: Xpress
(CARMA1)
Vector
wt
1-742
1-660
CD26 wt
(V5-tag)
kDa
Blot: anti-V5
(CD26 wt)
100
150
anti-Xpress
(CARMA1)
100
75
Lysate
anti-V5
Lane 1 2 3 4

Figure 6

A

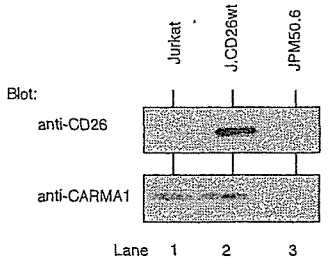

B

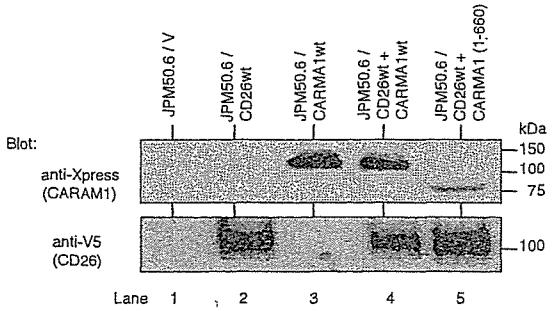

C

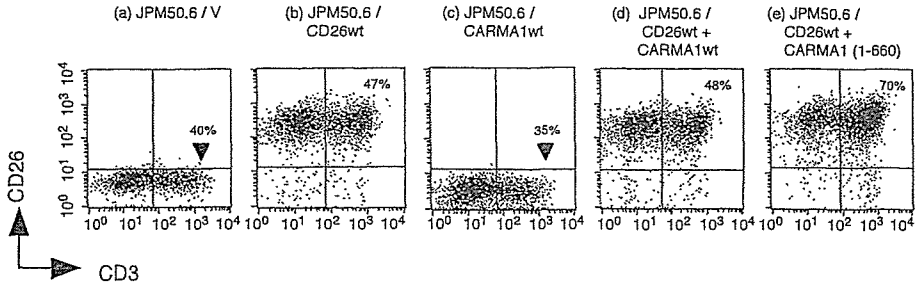

D

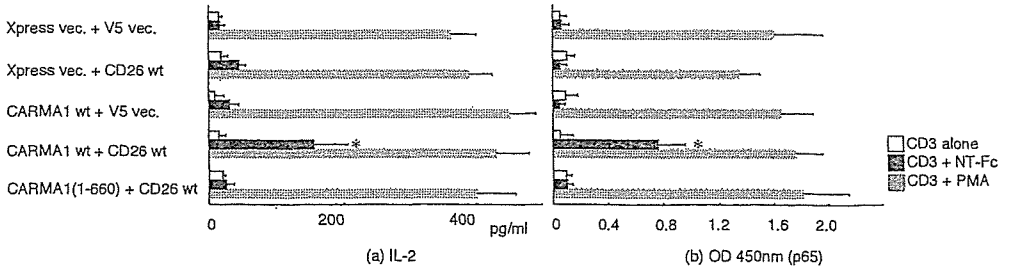

Figure 7

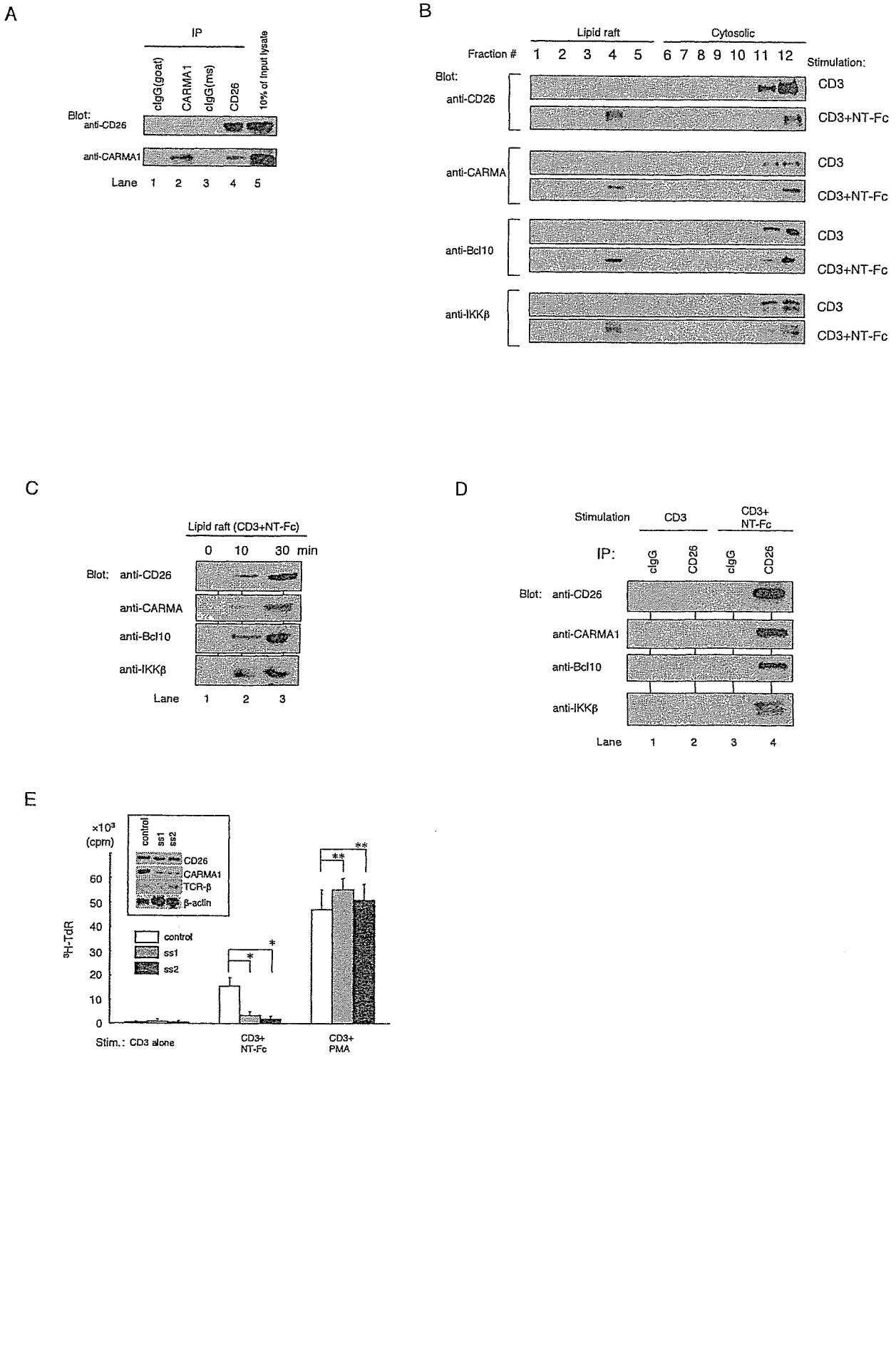
A
IP
cIgG(goat)
CARMA1
cIgG(ms)
CD26
10% of Input lysate
Blot:
anti-CD26
anti-CARMA1
Lane 1 2 3 4 5
B
Lipid raft
Cytosolic
Fraction # 1 2 3 4 5 6 7 8 9 10 11 12
Stimulation:
Blot:
anti-CD26
anti-CARMA
anti-Bcl10
anti-IKKβ
CD3
CD3+NT-Fc
C
Lipid raft (CD3+NT-Fc)
0 10 30 min
Blot: anti-CD26
anti-CARMA
anti-Bcl10
anti-IKKβ
Lane 1 2 3
D
Stimulation
CD3
CD3+ NT-Fc
IP:
cIgG
CD26
Blot: anti-CD26
anti-CARMA1
anti-Bcl10
anti-IKKβ
Lane 1 2 3 4
E
×10³ (cpm)
control
ss1
ss2
CD26
CARMA1
TCR-β
β-actin
³H-TdR
Stim.: CD3 alone
CD3+ NT-Fc
CD3+ PMA

Figure 8

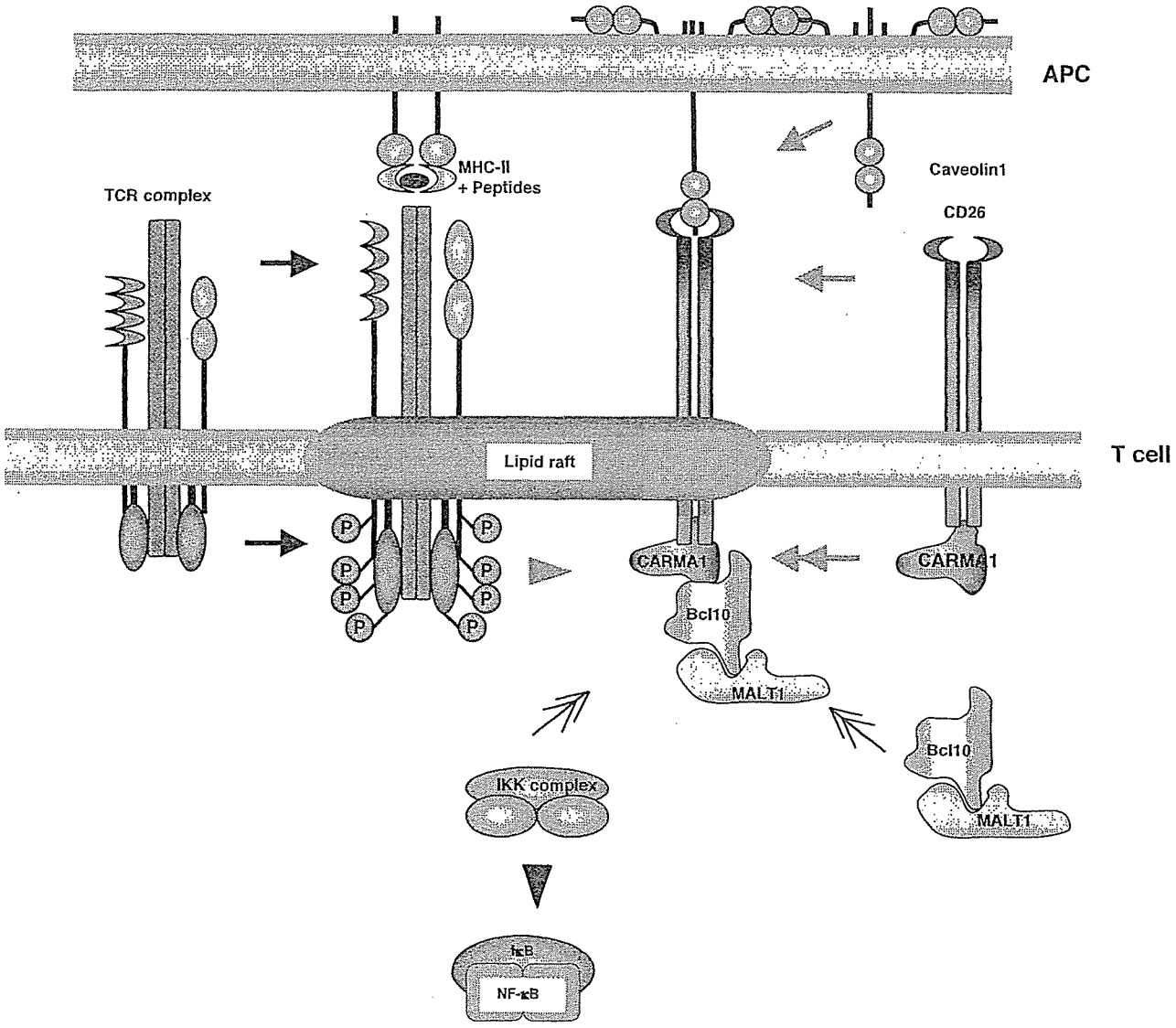
APC
MHC-II
+ Peptides
TCR complex
Caveolin1
CD26
Lipid raft
T cell
P
CARMA1
CARMA1
Bcl10
MALT1
Bcl10
MALT1
IKK complex
IκB
NF-κB

CD26/Dipeptidyl Peptidase IV as a Novel Therapeutic Target for Cancer and Immune Disorders

Michael A. Thompson[1], Kei Ohnuma[2], Masako Abe[3], Chikao Morimoto[2] and Nam H. Dang[3,*]

[1]*Division of Cancer Medicine, University of Texas M. D. Anderson Cancer Center, Houston, TX, USA;* [2]*Division of Clinical Immunology, Advanced Clinical Research Center, Institute of Medical Sciences, University of Tokyo, Tokyo, Japan;* [3]*Department of Hematologic Malignancies, Nevada Cancer Institute, Las Vegas, NV, USA*

Abstract: CD26 is a 110 kDa surface glycoprotein with intrinsic dipeptidyl peptidase IV (DPPIV) activity that is expressed on numerous cell types and has a multitude of biological functions. An important aspect of CD26 biology is its peptidase activity and its functional and physical association with molecules with key roles in various cellular pathways and biological programs. CD26 role in immune regulation has been extensively characterized, with recent findings elucidating its linkage with signaling pathways and structures involved in T-lymphocyte activation as well as antigen presenting cell-T-cell interaction. Recent work also suggests that CD26 has a significant role in tumor biology, being both a marker of disease behavior clinically as well as playing an important role in tumor pathogenesis and development. In this paper, we will review emerging data that suggest CD26 may be an appropriate therapeutic target for the treatment of selected neoplasms and immune disorders. Through the use of various experimental approaches and agents to influence CD26/DPPIV expression and activity, such as anti-CD26 antibodies, CD26/DPPIV chemical inhibitors, siRNAs to inhibit CD26 expression, overexpressing CD26 transfectants and soluble CD26 molecules, our group has shown that CD26 interacts with structures with essential cellular functions. Its association with such key molecules as topoisomerase IIα, p38 MAPK, and integrin β1, has important clinical implications, including its potential ability to regulate tumor sensitivity to selected chemotherapies and to influence tumor migration/metastases and tumorigenesis. Importantly, our recent *in vitro* and *in vivo* data support the hypothesis that CD26 may indeed be an appropriate target for therapy for selected cancers and immune disorders.

Key Words: CD26, dipeptidyl peptidase IV (DPPIV, DPP4), adenosine deaminase (ADA), autoimmune, T-cell.

1. INTRODUCTION

CD26 was described in 1966 as an enzyme with intrinsic dipeptidyl peptidase IV (DPPIV, EC 3.4.14.5) activity [1]. CD26/DPPIV selectively removes the N-terminal dipeptide from peptides with Pro or Ala in the third amino acid position (NH_2-X-X-↓-Ala/Pro-X...), where X is any amino acid and ↓ indicates the splice site [2]. DPPIV was later found to be the same as CD26, which is a 110 kDa extracellular membrane-bound glycoprotein that is expressed on numerous cell types and has a multitude of biological functions. Morrison *et al.* showed that adenosine deaminase (ADA)-binding protein-2 is identical to CD26 [3]. CD26 is a multifunctional type II transmembrane Ser peptidase that has an extracellular domain with DPPIV enzymatic activity and a short cytoplasmic domain. It interacts with extracellular molecules and is also involved in intracellular signal transduction cascades.

CD26 is important in immunology, autoimmunity, HIV, diabetes, and cancer. Interacting directly with various other cell surface and intracellular molecules, CD26 can regulate receptor specificity *via* its DPPIV activity and the function of various chemokines and cytokines. CD26 is expressed at low density on resting T-cells, but is upregulated with T-cell activation. Therefore, CD26 may have an important functional role in T-cells and overall immune function. CD26 associates with other important immunologic cell surface receptors such as CD45 and ADA. The multifunctional activities of CD26 are dependent on cell type and intracellular or extracellular conditions that influence its role as a proteolytic enzyme, cell surface receptor, co-stimulatory interacting protein and signal transduction mediator; as well as its role in adhesion and apoptosis. CD26/DPPIV has been the subject of recent reviews by Fleischer, 1995 [4], De Meester *et al.*, 1999 [5], Kahne *et al.*, 1999 [6], Hildebrandt *et al.*, 2000 [7], Gorrell *et al.*, 2001 [8], Langner and Ansorge, 2000 [9] and 2002 [10], Boonacker and Van Noorden, 2003 [11], as well as by our group [12-16]. In this review we stress the importance of CD26 in clinical conditions including various cancers and recent laboratory developments that elucidate its potential role as a novel therapeutic target.

2. STRUCTURE

CD26 is in the prolyl oligopeptidase/S9 enzyme family, which is characterized by a Ser-Asp-His catalytic triad in the C-terminal region. In humans and most mammals, the prolyl oligopeptidase gene family includes: prolyl endopeptidase (PEP), acylaminoacyl peptidase (ACPH), CD26/DPPIV, and three proteins highly related to CD26 -- fibroblast activation protein (FAP), DPPX, and DPP10 – as well as proteins with lower homology to CD26 -- DPP8 and DPP9. These proteins have moderate amino acid homology, but highly conserved structural features [17]. This includes higher conservation in

*Address correspondence to this author at the Department of Hematologic Malignancies, Nevada Cancer Institute, 10441 W. Twain Avenue, Las Vegas, NV 89135, USA; Tel: 702-822-5468; Fax: 702-944-2373;
E-mail: ndang@nvcancer.org

1389-5575/07 $50.00+.00

the C-terminal (an α/β-hydrolase domain) than in the N-terminus (a β-propeller region) [18]. The N-terminus also contains the consensus sequence (DW(V/L)YEEE), and the first two Glu (E) amino acids in this sequence are necessary for enzyme activity [19].

According to the HUGO Gene Nomenclature Committee (www.gene.ucl.ak./nomenclature/), the official gene symbol for CD26 is DPP4 and the official name is dipeptidyl-peptidase 4. The CD26 gene is located on chromosome 2q24.3 [20]. The gene is 70 kb and contains 26 exons, ranging from 45 to 1.4 kb in length [20]. The 5'-flanking region does not contain a TATA box or CAAT box, commonly found in housekeeping genes. CD26 does contain a 300 bp G-C rich region with potential binding sites for NFκB, AP2, or Sp1 [21]. CD26 expression is activated by interferons and retinoic acid in chronic lymphocytic leukemia (CLL) *via* Stat1α and the GAS response element (TTCnnnGAA located at bp -35 to -27) in the CD26 promoter [22]. A hepatocyte nuclear factor 1 binding site at position -150 to -131 of the CD26 gene regulates CD26 expression in human intestinal (Caco-2) and hepatic epithelial (HepG2) cell lines. Mutation of the CD26 promoter by the site directed mutagenesis approach resulted in transcription levels of 5-10% of the activity of the non-mutated controls [23]. The Ser recognition site (G-W-S-Y-G) is split between exons 21 and 22 (Fig. **1**). This differentiates CD26 from DPP8 and DPP9 – the putative ancestral genes for CD26/DPPIV/DPP4 in humans – which contain the Ser recognition site in one exon [18]. The CD26 cDNA contains a 3465 bp open reading frame that encodes a 766 amino acid protein [24]. The CD26 amino acid sequence has 85% amino acid identity with the mouse and rat CD26 genes and 37% amino acid identity with *D. melanogaster* (See Table **1** for other species). Chihara *et al.* recently characterized the *D. melanogaster* gene *omega*, one of five putative DPPIV genes, and described the evolutionary relationships of human DPPIV with other members of the prolyl oligopeptidase/S9 enzyme family [25]. Abbott *et al.* found two CD26 transcripts (4.2 and 2.8 kb), both of which were expressed at high levels in the placenta and kidney and at moderate levels in the lung and liver [20]. However, only the 4.2 kb mRNA was expressed at low levels in skeletal muscle, heart, brain, and pancreas.

CD26 has a short (6 amino acid) cytoplasmic domain, a transmembrane region, and an extracellular domain with DPPIV activity (Fig. **1** and Table **2**). The three-dimensional crystal structure of CD26 was determined from porcine kidney at a resolution of 1.8 Å [26]. The crystal structure of recombinant human CD26 was determined in the dimeric state at 2.5 Å resolution with the inhibitor Val-pyrrolidide (Fig. **2**) [27]. The last C-terminal 200 amino acids are similar to those of structural homologs prolyl oligopeptidase and proline imidopeptidase, which contain an α/β-hydrolase fold. It is interesting to note that the Pro residues are the only cyclic amino acids and may effect the susceptibility of proximal peptide bonds to cleavage [28, 29]. The catalytic site (Ser630-Asp708-His740) is located in a large cavity (also called a central tunnel), formed between the α/β-hydrolase domain and eight-bladed β-propeller domain, which contains the consensus sequence (DW(V/L)YEEE), that is common to S9b proteases [19, 27]. Single amino acid point mutations in the β-propeller motif identified Glu205 and Glu206 as essential for DPPIV enzyme activity [19]. The central tunnel and α/β-hydrolase domains both participate in inhibitor binding. This is not seen in classic Ser proteases in the chymotrypsin and subtilisin families [30, 31]. The propeller domain excludes large peptides occupying the catalytic pocket by steric hindrance, so there is only oligopeptidase (not polypeptidase) activity. The catalytic site is in the center of the lower face of the β propeller. The amino acids lining the opening to the catalytic site pocket control substrate specificity [32]. Boonacker and Van Noorden extensively review CD26 structure or activity homologs [11]. Substrate-assisted catalysis is one proposed mechanism for CD26/DPPIV substrate specificity [33].

3. EXPRESSION

CD26 is expressed in many tissues. Abbott *et al.* found two CD26 transcripts (4.2 and 2.8 kb), both of which were expressed at high levels in the placenta and kidney and at moderate levels in the lung and liver [20]. The 4.2 kb transcript was expressed at low levels in skeletal muscle, heart, brain, and pancreas [20]. Other organs expressing CD26 include: brain, endothelium [34], heart [20], intestine (colon adenocarcinoma, fetal colon expression disappears at birth) [3], kidney [3, 35], liver [3], lung [20], skeletal muscle [20], pancreas [20], and placenta [20]. In the hematopoietic system CD26 is found on CD4+ T memory cells, T-cells in lymphoblastic lymphoma (LBL), acute lymphoblastic leukemia (ALL), CD30+ anaplastic large cell lymphoma (ALCL), and T-large granular lymphocyte leukemia (T-LGLL). Soluble CD26 is found in serum. Expression of CD26 and CD40 ligand in the hematologic malignancies appears to be mutually exclusive [36, 37].

3.1. CD26 Isoforms

Kahne *et al.* have described various CD26 isoforms, some of which are associated with cell activation [38]. They found at least 5 enzymatically active DPPIV isoforms in activated lymphocytes and 11 immunoreactive DPPIV isoforms with isoelectric points between pH 3.5 and 5.9. Other isoelectric focusing studies have also demonstrated isoforms of CD26 [38-41]. Schmauser *et al.* showed with a series of experiments that purified CD26 consisted of several proteins with isoelectric points from 5.5 to 7.0 [41]. *In vitro* desialylation of CD26 followed by both isoelectric focusing and SDS-PAGE showed that isoelectric points were due to differences in the degree of sialylation [41]. Lectin affinity blotting with Sambucus nigra agglutinin and Maackia amurensis agglutinin revealed that CD26 was predominantly sialylated *via* an alpha 2,6-linkage. DPPIV activity is found only in basic isoforms not in acidic isoforms. A switch to acidic CD26 isoforms has been observed with HIV infection [40]. Neuraminidase treatment of HIV+ subject T-cells cleaves sialic acid residues and reduces the amount of acidic isoforms of CD26/DPPIV [40]. Mavropoulos *et al.* found a change in CD26 isoforms from acidic to a more neutral isoelectric point after anti-tumor necrosis factor-alpha therapy for rheumatoid arthritis [42]. Following cell mitogenic stimulation, one isoform may translocate from the cytoplasm to the cell surface membrane, which suggests isoform specific functions associated with cellular activation [38].